

# Dichotomy of Action-Potential Backpropagation in CA1 Pyramidal Neuron Dendrites

NACE L. GOLDING,<sup>1</sup> WILLIAM L. KATH,<sup>1,2</sup> AND NELSON SPRUSTON<sup>1</sup>

<sup>1</sup>*Department of Neurobiology and Physiology, Institute for Neuroscience and* <sup>2</sup>*Department of Engineering Sciences and Applied Mathematics, Northwestern University, Evanston, Illinois 60208*

Received 20 February 2001; accepted in final form 3 August 2001

**Golding, Nace L., William L. Kath, and Nelson Spruston.** Dichotomy of action-potential backpropagation in CA1 pyramidal neuron dendrites. *J Neurophysiol* 86: 2998–3010, 2001; 10.1152/jn. In hippocampal CA1 pyramidal neurons, action potentials are typically initiated in the axon and backpropagate into the dendrites, shaping the integration of synaptic activity and influencing the induction of synaptic plasticity. Despite previous reports describing action-potential propagation in the proximal apical dendrites, the extent to which action potentials invade the distal dendrites of CA1 pyramidal neurons remains controversial. Using paired somatic and dendritic whole cell recordings, we find that in the dendrites proximal to 280  $\mu\text{m}$  from the soma, single backpropagating action potentials exhibit  $<50\%$  attenuation from their amplitude in the soma. However, in dendritic recordings distal to 300  $\mu\text{m}$  from the soma, action potentials in most cells backpropagated either strongly (26–42% attenuation;  $n = 9/20$ ) or weakly (71–87% attenuation;  $n = 10/20$ ) with only one cell exhibiting an intermediate value (45% attenuation). In experiments combining dual somatic and dendritic whole cell recordings with calcium imaging, the amount of calcium influx triggered by backpropagating action potentials was correlated with the extent of action-potential invasion of the distal dendrites. Quantitative morphometric analyses revealed that the dichotomy in action-potential backpropagation occurred in the presence of only subtle differences in either the diameter of the primary apical dendrite or branching pattern. In addition, action-potential backpropagation was not dependent on a number of electrophysiological parameters (input resistance, resting potential, voltage sensitivity of dendritic spike amplitude). There was, however, a striking correlation of the shape of the action potential at the soma with its amplitude in the dendrite; larger, faster-rising, and narrower somatic action potentials exhibited more attenuation in the distal dendrites (300–410  $\mu\text{m}$  from the soma). Simple compartmental models of CA1 pyramidal neurons revealed that a dichotomy in action-potential backpropagation could be generated in response to subtle manipulations of the distribution of either sodium or potassium channels in the dendrites. Backpropagation efficacy could also be influenced by local alterations in dendritic side branches, but these effects were highly sensitive to model parameters. Based on these findings, we hypothesize that the observed dichotomy in dendritic action-potential amplitude is conferred primarily by differences in the distribution, density, or modulatory state of voltage-gated channels along the somatodendritic axis.

## INTRODUCTION

Neuronal dendrites mediate the conversion of complex spatial and temporal patterns of synaptic potentials into patterns of

action-potential output that convey the salient features encoded in presynaptic activity. In most mammalian central neurons, action potentials are initiated in the axon and propagate distally (“backpropagate”) into the dendritic arbor (Stuart et al. 1997b). The degree to which backpropagating action potentials invade the dendritic arbor depends critically on the dendritic morphology of neurons, which includes the parameters such as dendritic diameter and the pattern of dendritic branching (Goldstein and Rall 1974; Vetter et al. 2000). The efficacy of action-potential backpropagation also depends on the relative density of inward and outward currents activated by the backpropagating action potential. In Purkinje neurons, where the density of dendritic voltage-gated sodium channels decreases sharply with distance from the soma, action-potential backpropagation is nearly passive (Llinás and Sugimori 1980; Stuart and Häusser 1994), whereas in neurons where the ratio of dendritic sodium to potassium current is higher, backpropagation is nearly fully regenerative (mitral cells: Bischofberger and Jonas 1997; Chen et al. 1997; substantia nigra neurons: Häusser et al. 1995; hippocampal alveus-oriens interneurons: Martina et al. 2000).

The dendritic depolarization provided by backpropagating action potentials triggers calcium influx through voltage-gated calcium channels located on both dendritic shafts (Callaway and Ross 1995; Christie et al. 1996; Jaffe et al. 1992; Spruston et al. 1995; Svoboda et al. 1997) and spines (Koester and Sakmann 1998; Yuste and Denk 1995). Dendritic calcium influx arising from the coincidence of repetitive patterns of backpropagating action potentials and synaptic input has been shown to be critical for the induction of some forms of synaptic plasticity (reviewed in Linden 1999). In addition, dendritic calcium influx induced by high-frequency trains of backpropagating action potentials has also been shown to increase the efficacy of action-potential backpropagation itself (Tsubokawa et al. 2000).

In hippocampal CA1 pyramidal neurons, voltage-gated sodium channels are distributed along the somatodendritic axis at relatively uniform density (Magee and Johnston 1995), and activation of these channels by backpropagating action potentials limits the attenuation of the action potential as it propagates distally (Spruston et al. 1995). Active backpropagation of dendritic action potentials is highly activity dependent; during

Address for reprint requests: N. L. Golding, Dept. of Neurobiology and Physiology, Northwestern University, 2153 N. Campus Dr., Evanston, IL 60208-3520.

The costs of publication of this article were defrayed in part by the payment of page charges. The article must therefore be hereby marked “advertisement” in accordance with 18 U.S.C. Section 1734 solely to indicate this fact.

repetitive firing, backpropagating action potentials undergo a rapid, progressive decline in amplitude (Andreasen and Lambert 1995; Callaway and Ross 1995; Spruston et al. 1995), reflecting the cumulative inactivation of inward sodium current in the face of an activity-insensitive outward potassium current (Colbert et al. 1997; Jung et al. 1997; Mickus et al. 1999). Thus the degree of active invasion of the distal dendrites by backpropagating action potentials is dependent on both the frequency and temporal pattern of prior action-potential firing.

The extent to which action potentials invade the distal apical dendritic arbor of CA1 pyramidal neurons remains uncertain. The occurrence of major branch points in distal dendrites also makes it unclear whether differences in distal backpropagation efficacy reflect morphological versus physiological differences between cells. We have examined this issue by combining paired somatic and dendritic whole cell recordings with calcium-imaging techniques, quantitative anatomical analyses, and compartmental modeling. By restricting recordings to distal dendrites of consistent morphology, we have also attempted to assess the extent to which physiological differences between neurons influences the efficacy of action-potential backpropagation.

## METHODS

### *Slice preparation*

Hippocampal slices were prepared from male Wistar rats of postnatal ages 32–70 days. Following halothane anesthesia, rats were perfused transcardially with ice-cold artificial cerebrospinal fluid (ACSF) and decapitated, and the brain was removed. Hippocampal slices (300  $\mu\text{m}$  thickness) were then cut in ice-cold ACSF using an oscillating tissue slicer (Leica VT100, Nussloch, Germany). Slices were allowed to recover in a holding chamber for  $\sim 30$  min at  $35^\circ\text{C}$  and then at room temperature. For physiological recordings, slices were transferred to a recording chamber and maintained at  $33$ – $36^\circ\text{C}$ . During simultaneous recordings from the soma and distal dendrites  $>300$   $\mu\text{m}$  from the soma, the temperature was maintained between  $34$  and  $35^\circ\text{C}$ . Pyramidal neuron somata and dendrites were visualized on a fixed-stage microscope (Zeiss Axioscop2, Oberkochen, Germany) using infrared differential interference contrast videomicroscopy and a Newvicon camera (C2400, Hamamatsu, Hamamatsu City, Japan). ACSF was used for perfusion, dissection, and physiological recordings and contained (in mM) 125 NaCl, 25 glucose, 25  $\text{NaHCO}_3$ , 2.5 KCl, 1.25  $\text{NaH}_2\text{PO}_4$ , 2  $\text{CaCl}_2$ , and 1  $\text{MgCl}_2$  (pH 7.4, bubbled with 95%  $\text{O}_2$ -5%  $\text{CO}_2$ ).

### *Electrophysiology*

Simultaneous whole-cell current-clamp recordings were made using a pair of BVC-700 amplifiers (Dagan, Minneapolis, MN), using both bridge balance and capacitance compensation. Patch electrodes were fabricated from thick-walled borosilicate glass (EN-1; Garner Glass, Claremont, CA) and fire-polished on a microforge. Somatic and dendritic pipettes had open-tip resistances of 2–4 and 6–11  $\text{M}\Omega$ , respectively. Measurements of action-potential amplitude were made generally during the first 15 min of intracellular recordings, prior to extensive intracellular dialysis. Data from electrophysiological recordings were accepted if the series resistance remained  $<50$   $\text{M}\Omega$ . The intracellular pipette solution contained (in mM) 115 potassium gluconate, 20 KCl, 10 sodium phosphocreatine, 10 HEPES, 4 MgATP, 0.3  $\text{Na}_2\text{GTP}$ , 0.1% biocytin, and 2 EGTA. In a subset of electrophysiological experiments, potassium methylsulfate (115 mM) was used instead of potassium gluconate ( $n = 23$ ). For calcium imaging experiments, the preceding gluconate-based solution was

used, with 150  $\mu\text{M}$  Fura-2 or 150  $\mu\text{M}$  Bis-Fura-2 (Molecular Probes, Eugene, OR) substituting for EGTA.

Electrophysiological records were acquired using a Power Macintosh computer or Micron PC in conjunction with either an ITC16 or ITC18 computer interface (Instrutech; Port Washington, NY). Stimulus generation, data acquisition, and analysis were performed using custom macros written in IGOR Pro (Wavemetrics, Lake Oswego, OR). Electrophysiological records were filtered at 5 kHz and sampled at 50 kHz. Pooled data from electrophysiological recordings are expressed as means  $\pm$  SE. Unless otherwise noted, statistical significance was determined using Student's *t*-test with a significance level of 0.05.

### *Histology*

Cells were labeled by including 0.1% biocytin in internal pipette solutions. To maintain morphological integrity of recorded cells, recordings were terminated by gentle retraction of the patch pipette, forming an outside-out patch. The slice was then fixed in 4% paraformaldehyde and stored for 1–14 days at  $4^\circ\text{C}$ . To visualize labeled neurons, slices were reacted with the avidin-biotinylated horseradish peroxidase (HRP) complex (Vector Laboratories, Burlingame, CA) in conjunction with 3,3'-diaminobenzidine (Sigma, St. Louis, MO).

For Sholl analysis (Sholl 1953), reconstructions of pyramidal neurons were made at  $\times 20$  magnification using a *camera lucida* and then were scanned into a computer. Concentric circles with radii of multiples of 20  $\mu\text{m}$  were centered on the middle of the soma, and the number of dendritic crossings of each circle was determined manually.

For measurements of dendritic diameters and axonal lengths, pyramidal cells were visualized at  $\times 100$  (dendrites) and  $\times 20$  (axons), and measurements were made from images acquired with a CCD camera (Dage MTI, Michigan City, IN) in conjunction with ImagePro Plus software (Media Cybernetics, Silver Springs, MD). The number of oblique branches emanating from the primary apical dendrite was also determined at  $\times 100$  magnification.

### *Calcium imaging*

Cells filled with 150  $\mu\text{M}$  Fura-2 or Bis-Fura-2 were excited at 380 nm with a Mercury arc lamp (Zeiss) coupled to a liquid light guide (Sutter Instruments, Novato, CA). Emitted light was band-pass filtered at  $510 \pm 40$  nm and collected with a back-thinned, frame-transfer, cooled CCD camera (Micromax EBFT512; Roper Scientific, Trenton, NJ). At  $\times 40$  magnification, the field of view of the camera was  $170 \times 170$   $\mu\text{m}$ , corresponding to 0.33  $\mu\text{m}$  per pixel. Image acquisition (20 Hz) was performed using Winview 2.4 software (Roper Scientific) and coordinated with electrophysiological stimuli using IGOR Pro software. Images were analyzed using custom macros programmed in IGOR Pro. Measurements of fluorescence changes were made from small dendritic regions of interest ( $\sim 5 \times 20$   $\mu\text{m}$ ). Average fluorescence changes in a region were corrected for background autofluorescence by subtracting the average fluorescence of a region of identical dimensions located well away from labeled dendrites (but in the same field of view) and at the same distance from the pyramidal cell layer as the dendritic region of interest. Fluorescence changes were calculated nonratiometrically as  $\Delta F/F$ , where  $\Delta F$  equals the time-dependent change in fluorescence and  $F$  equals the resting fluorescence. Bleaching of the dye during the course of single trials was negligible, so no correction was required. Fluorescence measurements were calculated from the average of 5–20 trials.

### *Compartmental modeling*

A multicompartmental model was constructed using the NEURON simulation environment (Hines and Carnevale 1997), and simulations were performed using an integration step of 25  $\mu\text{s}$ . A CA1 pyramidal

neuron was reconstructed with a  $\times 63$  objective in conjunction with a NeuroLucida system (version 2.1, MicroBrightField, Colchester, VT). The NeuroLucida files were converted to NEURON coordinates using the Neuroconvert program (version 2.0b4, D. Niedenzu and G. Klien, MPI für Medizinische Forschung, Heidelberg, Germany). Model parameters were based on previous studies (Mainen et al. 1995; Migliore et al. 1999). The intracellular resistivity ( $R_i$ ) was  $200 \Omega\text{cm}$ , membrane resistance, ( $R_m$ ) was  $40,000 \Omega\text{cm}^2$ , and membrane capacitance ( $C_m$ ) was  $0.75 \mu\text{F}/\text{cm}^2$ . These values rendered a membrane time constant of 30 ms and an input resistance of  $60 \text{M}\Omega$ . To correct for the presence of spines,  $C_m$  was increased by a factor of 2 and  $R_m$  decreased by a factor of 2 in compartments beyond  $100 \mu\text{m}$  from the soma. In all simulations, a resting potential of  $-65 \text{mV}$  was imposed.

The model possessed three conductances: a voltage-gated sodium conductance ( $g_{\text{Na}}$ ), a delayed rectifying potassium conductance [ $g_{\text{K(DR)}}$ ], and an A-type potassium conductance [ $g_{\text{K(A)}}$ ]. The biophysical parameters of these conductances were implemented as in Migliore et al. (1999) and were inserted in all compartments of the cell and distributed in the cells as described in RESULTS.

To generate action potentials in the model, an axon was attached with properties based on a previous modeling study (Mainen et al. 1995). It consisted of an axon hillock ( $10 \mu\text{m}$  length), that tapered from 4 to  $1 \mu\text{m}$  in  $1\text{-}\mu\text{m}$  increments. The hillock was followed by an unmyelinated initial segment ( $15\text{-}\mu\text{m}$  length,  $1 \mu\text{m}$  diam) and three myelinated segments ( $1.5\text{-}\mu\text{m}$  diam,  $100 \mu\text{m}$  in length each) separated by nodes of  $1\text{-}\mu\text{m}$  diameter and length. In myelinated segments, the  $C_m$  was  $0.075 \mu\text{F}/\text{cm}^2$  and  $R_m$  was  $50 \Omega\text{cm}^2$ . The basal dendrites,

axon hillock, initial segment, and internodal axonal regions possessed conductances identical to that in the soma. However, the last 20% of the initial segment had a hot spot of sodium channels 100 times the density of the soma. In addition, the nodes possessed a sodium conductance of  $50,000 \text{mS}/\text{cm}^2$  and an A-type potassium channel density 20% that of the soma.

## RESULTS

We performed simultaneous somatic and dendritic whole cell patch recordings to measure the degree to which action potentials attenuate as they propagate along the primary apical dendrites. Recordings were made from pyramidal neurons in the CA1 region of hippocampal slices. Trains of action potentials ( $10\text{--}20 \text{Hz}$ ) were triggered with depolarizing current steps (1-s duration) injected through the somatic recording pipette (Fig. 1A). These action potentials were always detected first at the soma and subsequently in the dendrite, consistent with their site of initiation being near or in the axon (Spruston et al. 1995). An activity-dependent attenuation of backpropagating action potentials was observed in dendritic recordings and appeared more marked the further the recording was from the soma (Fig. 1A), consistent with previous studies (Andreasen and Lambert 1995; Callaway and Ross 1995; Spruston et al. 1995). Figure 1B (left) shows the amplitude of the first back-

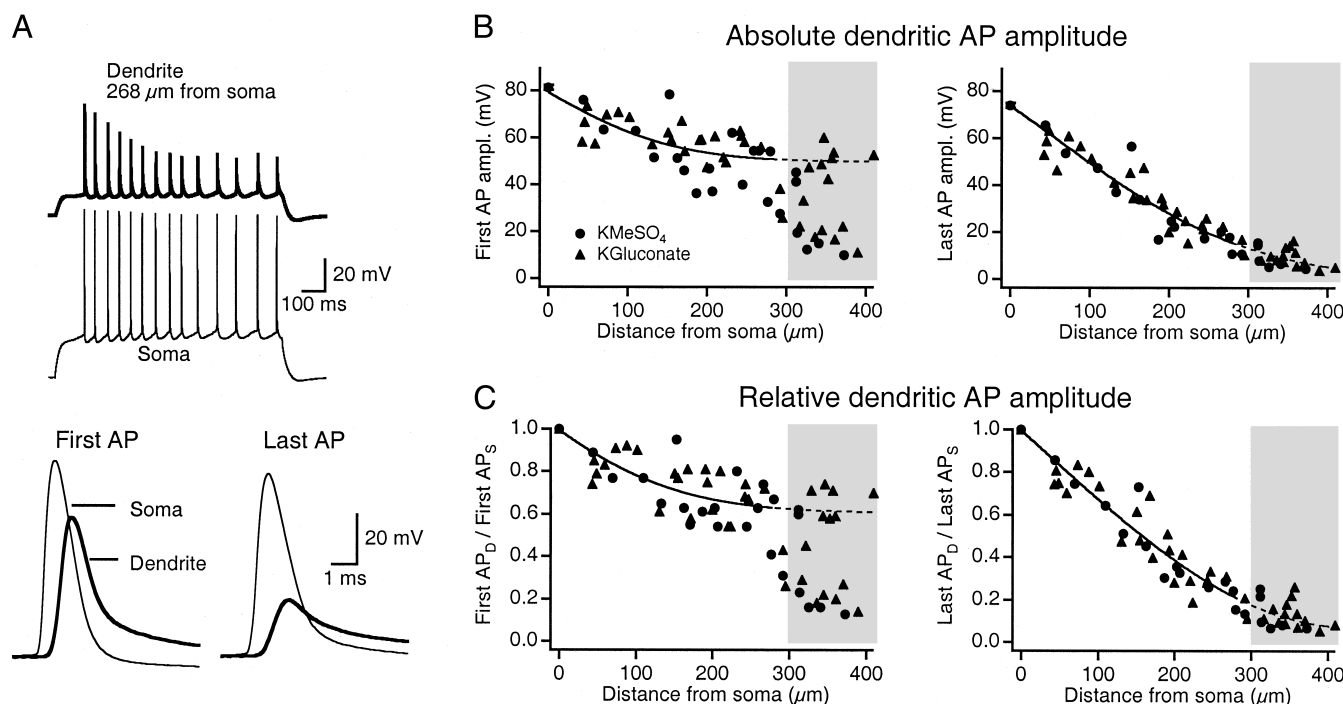


FIG. 1. Backpropagation of action potentials in dendrites. *A*: simultaneous whole cell patch-pipette recordings from the soma (light traces) and primary apical dendrite (dark traces) of a CA1 pyramidal neuron. A  $300\text{-pA}$  somatic depolarizing current pulse 1 s in duration triggers a train of action potentials that are detected in the soma and dendrite. Note the progressive decline of backpropagating action potentials in the dendrite. *Bottom*: expanded views of the 1st and last action potential in the train reveal that the action potential is recorded first at the soma and then subsequently in the dendrite, consistent with the interpretation that these action potentials were initiated in or near the axon. *B*: the amplitude of the 1st (left) and last (right) backpropagating action potentials in a 10- to 20-Hz train as a function of the distance they are recorded from the soma. In each graph, the data between 0 and  $280 \mu\text{m}$  was fit with a gaussian function (solid line), and extrapolated to  $410 \mu\text{m}$  (dashed line). Gaussian functions provided better fits than exponentials. At distances  $>300 \mu\text{m}$  from the soma (shaded area), a dichotomy in the amplitude of the 1st action potentials becomes apparent (left), with 19/20 cells exhibiting either strong ( $>40 \text{mV}$  amplitude) or weak propagation ( $<25 \text{mV}$  amplitude). By contrast, the amplitude of the last spike in a train declines monotonically (right). Points at  $0 \mu\text{m}$  represent the means  $\pm$  SE of 38 somatically recorded action potentials.  $\bullet$  and  $\blacktriangle$ , cells recorded with  $\text{KMeSO}_4$  and  $\text{KGluconate}$  internal solutions, respectively. *C*: similar plots as in *B*, only dendritic action-potential amplitude is plotted relative to the amplitude of the simultaneously recorded action potential at the soma. Fitting methods are identical to those in *B*.

propagating action potential in a train as a function of distance from the soma. Action potentials backpropagated with modest attenuation at distances  $<280 \mu\text{m}$  from the soma. Action potentials in this proximal region exhibited amplitudes  $>36 \text{ mV}$  (Fig. 1*B, left*), representing less than a 50% decline in amplitude relative to the amplitude of the action potential recorded simultaneously at the soma (Fig. 1*C, left*). In 20 dual somatic and dendritic recordings, however, backpropagating action potentials recorded beyond  $300 \mu\text{m}$  exhibited a dichotomy in their propagation efficacy. In 45% of these recordings, action potentials propagated strongly, showing 26–42% decline in amplitude ( $n = 9/20$ ). By contrast, in 50% of recordings, action potentials propagated weakly, exhibiting 71–87% attenuation ( $n = 10/20$  cells). An intermediate amplitude was observed in only one recording, accounting for 5% of the data obtained at distal locations. The amplitude of action potentials was stable during recordings, and cells never switched between weak and strong backpropagation.

In the dendrites distal to  $300 \mu\text{m}$  from the soma, the amplitude of the first backpropagating action potential elicited during 10- to 20-Hz trains was relatively insensitive to the rate of rise of the depolarization preceding the spike; single action potentials elicited with brief somatic current steps 5 ms in duration differed from those elicited during 1-s depolarizations in the same cells by only 0.5–3.7 mV, corresponding on average to a  $2.8 \pm 1.1\%$  difference in attenuation ( $n = 6$ ). Furthermore, backpropagating action-potential amplitude was similarly insensitive to differences in the timing of the spike during current steps 1 s in duration, where the first action potential occurred between 51 and 277 ms after the onset of the current pulse. The ages of animals from which distal recordings were made were not significantly different ( $51 \pm 2$  days for strong-propagating neurons,  $n = 9$ ;  $48 \pm 3$  days for weak-propagating neurons,  $n = 10$ ;  $t$ -test,  $P > 0.4$ ). Differences in action-potential invasion of the distal dendrites were also not accompanied by significant differences in average input resistance ( $45.7 \pm 1.5 \text{ M}\Omega$  in strong-propagating neurons,  $n = 6$ ;  $45.3 \pm 1.8$  in weak-propagating neurons,  $n = 4$ ;  $t$ -test,  $P > 0.8$ ).

The dichotomy in backpropagation efficacy was not observed after backpropagating action potentials had undergone activity-dependent amplitude attenuation following trains of prior action potentials (Fig. 1, *B* and *C, right*). The activity dependence of backpropagating action-potential amplitude reflects activity-dependent changes in the ratio of sodium to potassium current (Colbert et al. 1997; Jung et al. 1997; Mickus et al. 1999). The fact that the attenuation of distal backpropagating action potentials at the end of trains in all cells appears similar to the first action potential in weak-propagating pyramidal neurons suggests that the dichotomy in distal backpropagation efficacy across pyramidal neurons reflects, at least in part, differences in the degree of action-potential amplification by voltage-gated channels in the dendrites.

The efficacy of action-potential backpropagation in CA1 pyramidal neurons is known to be sensitive to the membrane potential at which they are evoked (Magee and Johnston 1997; Tsubokawa and Ross 1996), raising the possibility that resting potential variability across pyramidal neurons might impose a corresponding variability in action-potential backpropagation. However, the somatic and dendritic resting potentials of strong

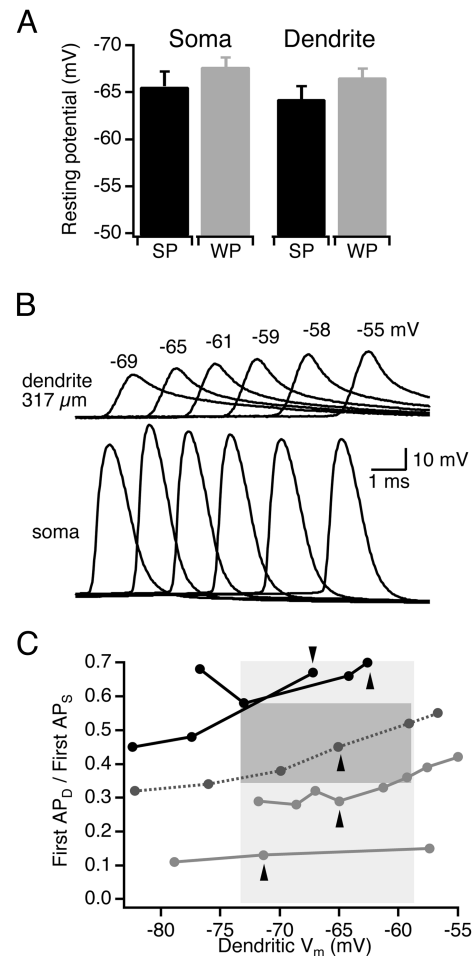


FIG. 2. Resting potential variability does not account for differences in the efficacy of action-potential backpropagation. *A*: Average resting potentials in the soma and distal dendrites ( $>300 \mu\text{m}$  from soma) are not significantly different (2-mV difference) in pyramidal cells exhibiting strong (SP,  $n = 9$ ) and weak (WP,  $n = 10$ ) action-potential backpropagation ( $t$ -test;  $P > 0.1$  for dendritic recordings,  $P > 0.2$  for somatic recordings). *B*: Action-potential backpropagation is voltage sensitive. During polarization of the membrane potential with dendritic current injection, backpropagating action potentials increased in amplitude when elicited from progressively more depolarized membrane potentials. By contrast, somatic action potentials showed a biphasic response to membrane polarization. The resting membrane potential of the cell was  $-65 \text{ mV}$  in the dendrite and  $-64 \text{ mV}$  at the soma. For clarity, action potentials are shown offset temporally from one another. *C*: Voltage sensitivity of backpropagating action-potential attenuation cannot account for the wide range of dendritic spike amplitudes observed in cells exhibiting different resting potentials. Each set of connected points corresponds to measurements from 1 cell in which direct hyperpolarizing or depolarizing current was injected through the dendritic electrode (between 317 and  $410 \mu\text{m}$  from the soma). Dark lines, SP; light lines, WP. Note that the voltage-dependent action-potential amplitudes from strong- and weak-propagating neurons are separated by a gap (darker shaded area) over the range of resting potentials observed in all 20 dual recordings distal to  $300 \mu\text{m}$  from the soma (lighter shaded area). Measurements from the 1 cell exhibiting intermediate action-potential attenuation fall within this gap and are shown connected by a dashed line. Measurements made at the resting potential of each cell are indicated with an arrowhead.

and weak-propagating pyramidal neurons varied only by an average of 2 mV and were not significantly different (Fig. 2*A*;  $t$ -test,  $P > 0.1$  for dendritic recordings;  $P > 0.2$  for somatic recordings). In five neurons, we measured the sensitivity of backpropagating action potentials to polarization of the membrane potential induced by constant dendritic current injection

(Fig. 2, *B* and *C*). Backpropagating action-potential amplitude always increased in response to steady depolarization and decreased in response to steady hyperpolarization of the membrane potential. However, hyperpolarization of the membrane potential of strong-propagating pyramidal neurons over the range of resting potentials encountered in this study did not decrease the amplitude of backpropagating action potentials to values observed in weak-propagating neurons. Conversely, depolarization of the dendritic membrane potential of weak-propagating pyramidal did not increase the amplitude of backpropagating action potentials to values observed in strong-propagating neurons (Fig. 2, *B* and *C*). These results indicate that although the amplitude of backpropagating action potentials is sensitive to membrane potential, variability in the resting potential among pyramidal neurons does not account for the dichotomy in amplitude of backpropagating action potentials.

The efficacy of distal backpropagation was correlated with the shape of the action potential recorded at the soma near the site of initiation. Weak-propagating pyramidal neurons exhibited somatic action potentials that tended to be larger, faster rising, and of narrower width than action potentials in strong-propagating neurons (Fig. 3, *A–C*). The scatter plots of the raw data reveal that the dichotomy in action-potential backpropagation was not accompanied by a similar dichotomy in any of the parameters of action-potential shape. Rather, action-potential shape parameters of strong- and weak-propagating pyramidal neurons occupied opposite ends of continuous distributions. Indeed, the maximum rate of rise and duration of action potentials were, with one exception, nonoverlapping in strong- and weak-propagating pyramidal neurons. Thus within the subpopulation of pyramidal neurons sampled in this study, strong and weak propagation efficacy can be predicted with high accuracy by the shape of the somatic action potential. The length of the axon in twelve biocytin-labeled cells exhibiting weak and strong backpropagating action potentials was  $\geq 94 \mu\text{m}$  and averaged  $549 \pm 191 \mu\text{m}$  ( $n = 6$ ) and  $1,030 \pm 232 \mu\text{m}$  ( $n = 6$ ), respectively (not significantly different;  $P > 0.05$ ,  $t$ -test). Because the site of action-potential initiation has been estimated to occur in the distal initial segment or first node of Ranvier ( $\sim 30 \mu\text{m}$  from the soma) (Colbert and Johnston 1996; Stuart et al. 1997a), it is unlikely that the observed differences in action-potential shape resulted from axotomy-induced differences in the number of axonal sodium channels contributing to action-potential generation. It is unclear whether the differences in action-potential shape are causally related to their eventual propagation efficacy in the distal dendrites. However, these findings provide strong support for heterogeneity in the density, distribution, or modulatory state of intrinsic ion channels in CA1 pyramidal neurons.

The attenuation of action potentials in dendrites is sensitive to dendritic diameter and branching structure (Vetter et al. 2000). To assess whether the differences in action-potential backpropagation across CA1 pyramidal neurons reflect differences in morphology, we examined the dendritic morphology of 12 biocytin-labeled pyramidal neurons in which recordings were made from the soma and apical dendrite  $>300 \mu\text{m}$  from the soma. Six of these neurons exhibited strong backpropagation, whereas six neurons exhibited weak backpropagation. These neurons were all located in the CA1 region away from

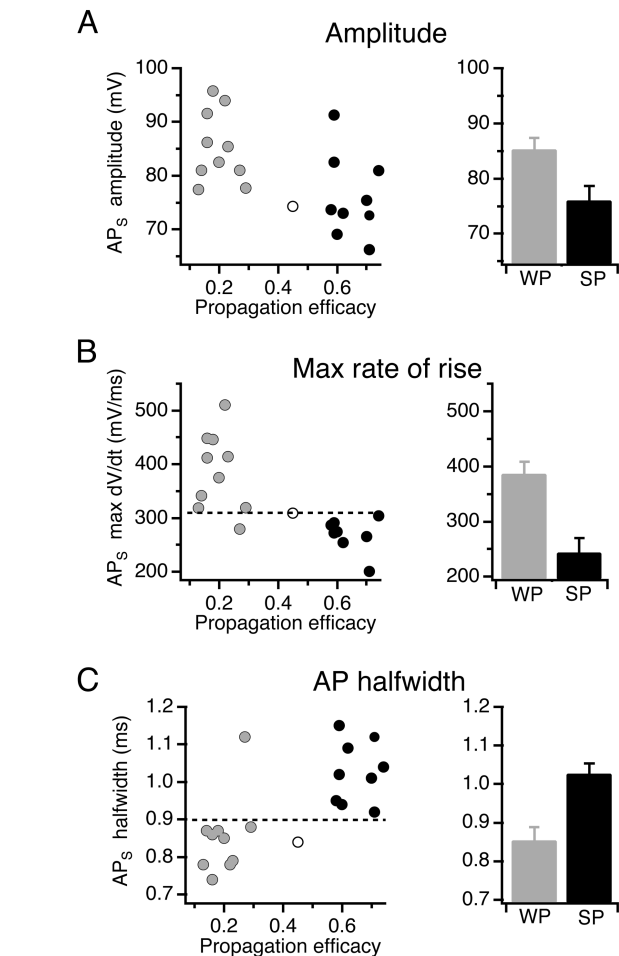


FIG. 3. The size and shape of the action potential is correlated with its efficacy of backpropagation. *A, left*: plot of somatic action-potential amplitude vs. propagation efficacy (the ratio of dendritic to somatic action-potential amplitude) shows that smaller somatic action potentials tend to propagate more effectively than larger ones. ●, strong propagating neurons (SP); ○, weak-propagating neurons (WP). ○, one cell that exhibited intermediate propagation efficacy. *Right*: average somatic action-potential amplitude in strong- and weak-propagating neurons is significantly different ( $t$ -test,  $P < 0.03$ ). *B*: strong-propagating action potentials have slower maximal rates of rise (given by the maximum in the derivative of the action potential) than weak-propagating action potentials. With one exception, strong- and weak-propagating neurons occupy nonoverlapping regions of the distribution (*left*, separated by  $\cdots$ ). *Right*: average maximal rate of rise of somatic action potentials in strong- and weak-propagating neurons is significantly different ( $t$ -test,  $P < 0.001$ ). *C*: strong-propagating action potentials are longer in duration, as given by the width of the action potential at half-amplitude. With one exception, strong- and weak-propagating neurons occupy nonoverlapping regions of the distribution (*left*, separated by  $\cdots$ ). *Right*: average width of somatic action potentials in strong- and weak-propagating neurons is significantly different ( $t$ -test,  $P < 0.003$ ).

the boundary region between CA1 and subiculum where the pyramidal cell layer appears less distinct. The somata of these neurons were displaced from the pyramidal cell layer, in stratum oriens, with the exception of one strong-propagating neuron whose soma was located in the pyramidal cell layer itself. Among the displaced neurons, there was no significant difference in the location of the somata of neurons exhibiting strong and weak backpropagation relative to the middle of the pyramidal cell layer ( $83 \pm 12$  vs.  $88 \pm 10 \mu\text{m}$  displacement, respectively;  $t$ -test,  $P > 0.7$ ). This recording bias enabled

unbranched primary apical dendrites of longer lengths to be followed in s. radiatum before they were obscured by their entry into the more heavily myelinated s. lacunosum-moleculare. Reconstructions made with a camera lucida of these pyramidal neurons revealed that all dendritic recordings were made from the primary apical dendrite prior to any major bifurcation (Fig. 4). Although there is some variability in dendritic morphology among cells, no obvious systematic differences in dendritic morphology are apparent. We examined the branching complexity of strong- and weak-backpropagating pyramidal neurons quantitatively, using Sholl analysis (Fig. 5A). The two distributions of dendritic complexity were not significantly different (Kolmogorov-Smirnov test;  $P > 0.5$ ). The total number of primary oblique branches was also not significantly different between strong- and weak-propagating neurons (Fig. 5C;  $t$ -test;  $P > 0.7$ ). However, there were small but consistent local differences in branching complexity in the region of the dendrites between 300 and 350  $\mu\text{m}$  from the soma (Fig. 5A), the region where the dichotomy in action-potential backpropagation becomes apparent. In this region, the number of primary oblique branches also differed by a small, but consistent amount (0 vs. 2 branches in strong- vs. weak-propagating neurons, respectively). Finally, no significant differences were observed in the diameter of the primary apical dendrite of cells in each group at distances  $\leq 350$   $\mu\text{m}$  from the soma, the longest distance in which no major bifurcations occurred in the sample of labeled pyramidal neurons (Fig. 5D). Based on these analyses, it is unlikely that gross morphological differences contributed substantially to the observed dichotomy in action-potential backpropagation efficacy, although local differences in branching structure cannot be discounted.

Backpropagating action potentials serve as potent sources of postsynaptic calcium influx and may play an important role in the induction of certain forms of synaptic plasticity (Linden 1999). We thus asked whether the differences in the backpropagation efficacy of action potentials imposed a similar dichotomy in the magnitude of postsynaptic calcium concentration changes in the dendrites. To address this question, we

combined simultaneous somatic and dendritic whole cell recordings with Fura-2 or Bis-Fura-2 calcium imaging. Single action potentials were generated with brief (5 ms) somatic current pulses, and the resultant fluorescence changes were measured in small ( $\sim 5 \times 20$   $\mu\text{m}$ ) regions of interest along the apical dendritic arbor. The amplitude of the spike-triggered calcium influx in the distal apical dendrite was correlated with the propagation efficacy of action potentials. In pyramidal neurons exhibiting large backpropagating action potentials in the distal dendrites, spike-triggered calcium influx declined little with distance along the primary apical dendrite (Fig. 6A;  $n = 2$ ). By contrast, in cells exhibiting small backpropagating action potentials in the distal dendrites, spike-triggered calcium influx declined considerably with distance along the apical dendrite (Fig. 6B;  $n = 2$ ). These findings are summarized in Fig. 7A, which shows the absolute calcium-dependent fluorescence changes measured along the apical dendrite in the population of imaged pyramidal neurons. When the calcium concentration changes in the distal dendrites are normalized to the maximum fluorescence changes (typically occurring between 200 and 250  $\mu\text{m}$  from the soma), a dichotomy in the data emerges (Fig. 7B). In one group of cells, intracellular calcium changes decline  $<20\%$  in the region between 300 and 450  $\mu\text{m}$ , whereas in another group of cells, calcium influx declines over 65% in the same distal region. In four of the seven experiments shown, the association of the magnitude of calcium influx with the strength of action-potential backpropagation was confirmed using dual somatic and dendritic whole cell recordings. Taken together, these results suggest that the profile of calcium influx along the dendrite is associated with the propagation efficacy of action potentials.

We constructed compartmental models of morphologically reconstructed CA1 pyramidal neurons to explore potential mechanisms controlling the amplitude of backpropagating action potentials in the dendrites. These models contained voltage-gated sodium channels as well as delayed-rectifying and A-type potassium channels. Weak action-potential backpropagation was exhibited by a model containing uniform distribu-

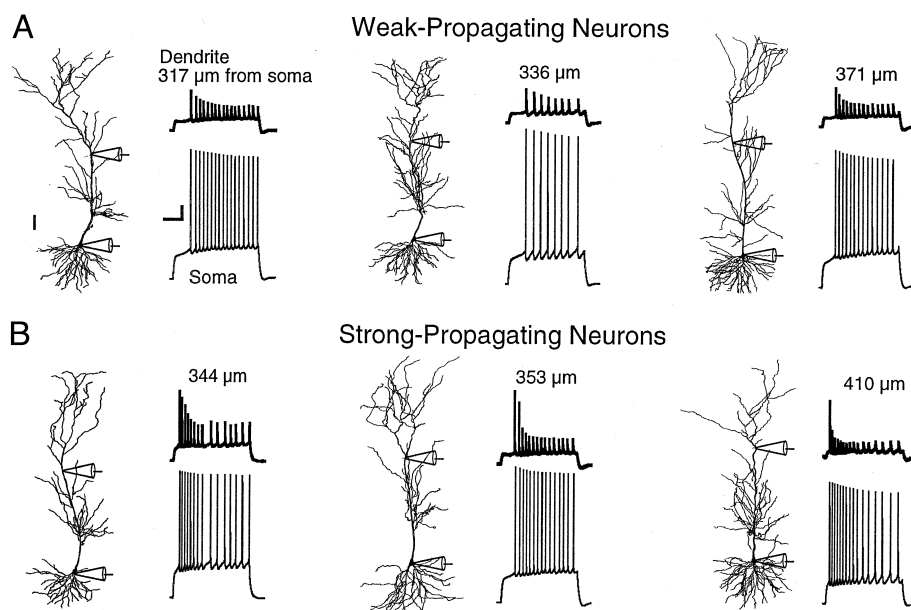


FIG. 4. Dichotomy in backpropagation efficacy is not associated with systematic differences in morphology. *A*: trains of action potentials are elicited in 3 biocytin-labeled pyramidal neurons in response to depolarizing current steps, 1 s in duration. Backpropagating action potentials appear highly attenuated in each distal dendritic recording. Morphology scale bar: 50  $\mu\text{m}$ . Physiology scale bar: 10 mV, 200 ms. *B*: responses of 3 different labeled pyramidal neurons to depolarizing current pulses. Trains of backpropagating action potentials are initially of large amplitude and show progressive attenuation. The overall morphology of these neurons appears similar to those shown in *A*. Scale is the same as in *A*.



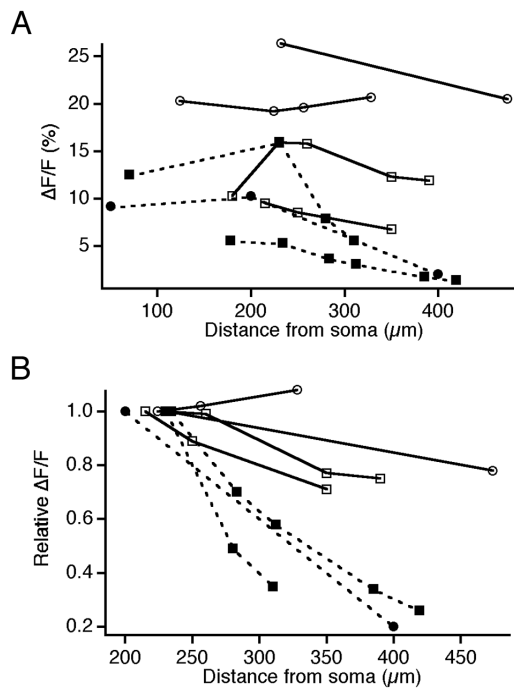


FIG. 7. Summary of calcium influx triggered by single backpropagating action potentials. *A*: single action-potential-induced calcium influx as a function of dendritic distance. Each set of connected points reflects measurements taken from a different neuron. Calcium influx decreased only modestly in some neurons (—) but more markedly in others (···). When imaging experiments were combined with simultaneous somatic and distal dendritic recordings, strong or weak distal calcium influx was always found to be associated with strong or weak action-potential backpropagation, respectively ( $\square$  and  $\blacksquare$ ,  $n = 4$ ).  $\bullet$  and  $\circ$  correspond to imaging experiments with single somatic recordings. *B*: action-potential-induced intracellular calcium concentration changes as a function of distance, normalized to the maximum calcium-induced fluorescence change (typically occurring in the dendrite between 200 and 250  $\mu\text{m}$  from the soma). While in many cells, action-potential-induced changes in calcium influx were reduced only modestly (<25%; —), in other neurons, large declines in action-potential-induced calcium influx were observed (>65% decline; ···). These corresponded to weak and strong backpropagating neurons, as described in *A*.

near the dendritic region where the dichotomy in action-potential backpropagation could first be distinguished (2 vs. 0 primary branches on average in weak- and strong-propagating neurons, respectively). Our compartmental model exhibited a similar region where backpropagation dichotomy emerged, although this region occurred somewhat more proximally than in the experimental data (Fig. 9, *A* and *B*, *right*). It is thus possible that appropriately located oblique branches could promote weak action-potential propagation by drawing current from the primary apical dendrite. We tested this possibility by removing distal dendritic branches from neuron models that exhibited weak action-potential backpropagation. Removal of small numbers of oblique branches in most of these models resulted in a small increase in backpropagating action-potential amplitude (a few millivolts). The magnitude of this effect was proportional to the diameter and length of the removed branch as well as its distance from the soma. However, removal of a small number of branches could convert a weak-propagating neuron to a strong one under optimal conditions. Figure 10 shows the effects of removing three branches from the primary apical

dendrite  $\sim 200 \mu\text{m}$  from the soma in three models incorporating different dendritic distributions of sodium channels. Branch removal could convert a weak-propagating neuron to a strong one only when the distribution of sodium and potassium channels yielded action potentials that propagated just below the threshold for active propagation (Fig. 10*B*). These results indicate that the presence or absence of large, strategically located dendritic side branches has the potential to influence the efficacy of action-potential backpropagation.

## DISCUSSION

Actively backpropagating action potentials communicate the firing activity of the axon to the dendritic arbor. The extent to which action potentials invade the distal dendrites is influenced by a complex set of parameters, which include the pattern and frequency of prior action-potential discharge, inhibition, and dendritic morphology. By combining simultaneous distal den-

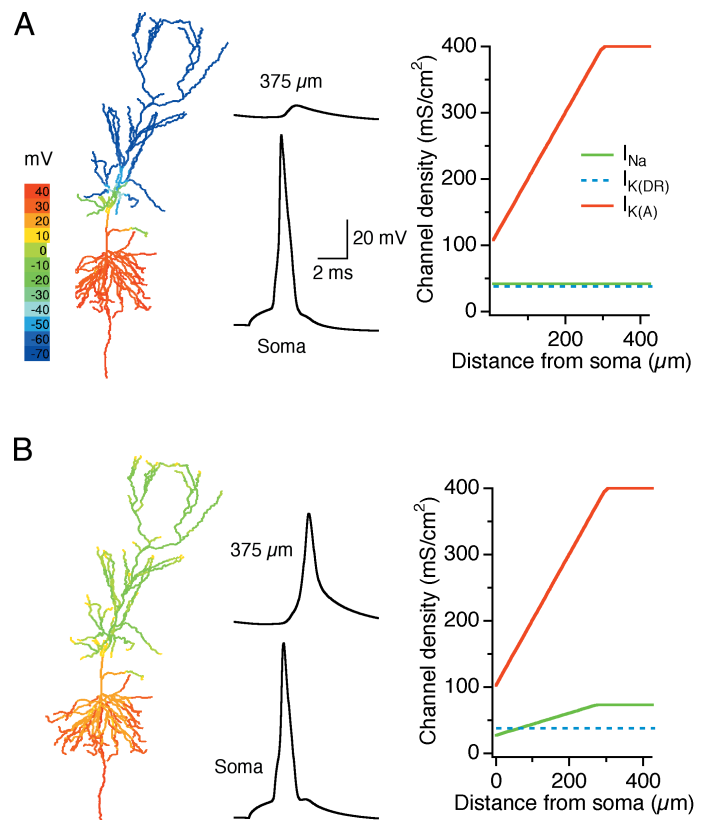


FIG. 8. Modeling strong and weak action-potential backpropagation. *A*: the spatial profile of action-potential amplitude in a model of a weak-propagating CA1 pyramidal cell. Peak action potential voltage is expressed relative to the resting potential ( $-65 \text{ mV}$ ) and is shown color-coded in the morphological reconstruction (*left*). Backpropagating action potentials, in the soma and dendrites 375  $\mu\text{m}$  away, were elicited by simulating somatic current injection (400-pA, 5-ms duration; *middle*). *Right*: model parameters, which consist of uniform distributions of sodium and delayed rectifying potassium channels and a gradient of A-type potassium channels that increases to four times the somatic density in the first 300  $\mu\text{m}$  of the apical dendrite. *B*: the spatial profile of action-potential amplitude in a model of a strong-propagating neuron. Figure format as in *A*. The action potential propagates effectively to the tips of the most distal apical dendrites. *Right*: the channel distributions were identical to those in the model shown in *A* with the exception that a slight positive gradient was introduced to the sodium channel density.

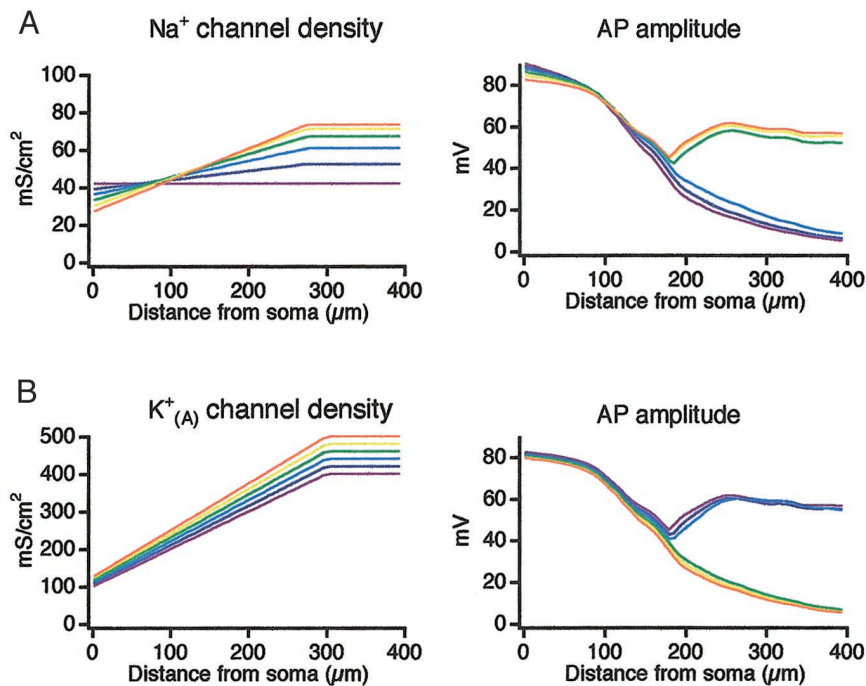


FIG. 9. Subtle changes in the distribution of sodium and A-type potassium channels can induce a dichotomy of action-potential backpropagation. *A*: sodium channels were distributed either uniformly or in weakly increasing dendritic gradients (*left*) in the face of constant potassium channel distributions. Models with uniform and weakly increasing sodium channel gradients (purple, blue, and turquoise lines) exhibited weakly propagating action potentials (*right*), whereas models with steeper gradients exhibited strongly propagating action potentials (green, yellow, and orange traces). Models with steeper gradients also had lower densities of sodium channels in the soma and proximal dendrites. Potassium channel distributions are identical to those in Fig. 8A under all conditions. *B*: the somatodendritic gradient of A-type potassium channels was varied (*left*), while the distribution of sodium channels was held constant. As the slope of the potassium channel gradient was increased, action-potential propagation changed from weak (orange, yellow, and green lines) to strong (turquoise, blue, and purple lines) with no intermediate values.

dratic and somatic whole-cell recordings with calcium imaging and quantitative anatomical analyses, we have shown in a morphologically homogenous population of pyramidal neurons that action-potential backpropagation in the distal dendrites exhibits a bimodal distribution. In 95% of these pyramidal neurons, backpropagation beyond 300  $\mu\text{m}$  from the soma appears either highly active, with action potentials exhibiting 26–42% attenuation, or nearly passive, with action potentials exhibiting 71–87% attenuation. The spatial profile of distal action-potential-triggered calcium influx exhibits a similar dichotomy. Although variability in dendritic complexity strongly influences the efficacy of action-potential backpropagation (Vetter et al. 2000), the cells in the present study were similar in overall morphology. However, the efficacy of action-potential backpropagation was correlated with the amplitude and kinetics of the somatic action potential. The shape of action potentials at the soma thus serves as a simple assay of backpropagation efficacy. These results, together with those from a compartmental model, support the hypothesis that the subunit expression, distribution, or modulatory state of voltage-gated channels can differ in individual CA1 pyramidal neurons and that such differences can give rise to functional diversity, even in morphologically similar pyramidal neurons.

#### Distal extent of action-potential invasion of the dendrites

There have been conflicting reports regarding the distal extent of action-potential backpropagation in the dendrites of CA1 pyramidal neurons. A previous study (Spruston et al. 1995) found that the action potentials propagated strongly, exhibiting <50% attenuation from the soma to the primary apical dendrite as far away as 400  $\mu\text{m}$ . Other studies have reported a wide range of amplitudes of backpropagating action potentials in the distal dendrites (Magee and Johnston 1995; Tsubokawa and Ross 1996, 1997; Tsubokawa et al. 2000).

Discrepancies between studies likely stem in part from differences in the temperature at which recordings were made ( $\sim 34^\circ\text{C}$  in the present study; room temperature in Spruston et al. 1995).

The age of animals may also influence the degree of action-potential backpropagation. The density of voltage-gated sodium channels in CA1 pyramidal neurons has been shown to increase between 3 and 5 wk of age (Magee and Johnston 1995). During the same period, the dendritic tree increases in size and complexity (Pokorny and Yamamoto 1981). While developmental changes in voltage-gated channels or dendritic morphology might contribute to differences in the degree of backpropagation in studies using animals of different ages, such changes are unlikely to explain the dichotomy in backpropagation observed in the present study because the average age as well as the overall range of ages of rats was similar in experiments where strong and weak backpropagation was observed.

A critical issue is whether backpropagating action potentials invade the distal dendritic arbor *in vivo*. Using sharp microelectrode recordings from CA1 pyramidal neurons in anesthetized rats, Kamondi et al. (1998) have examined the attenuation of spontaneous action potentials along the somatodendritic axis. Interestingly, they report that the amplitude of backpropagating action potentials drops precipitously at  $\sim 280 \mu\text{m}$  from the presumed location of the soma. This distance is remarkably similar to the dendritic location in the present study at which pyramidal neurons exhibiting strong and weak action-potential backpropagation begin to be distinguishable from one another. The fact that strong-propagating pyramidal neurons have not been observed *in vivo* might reflect differences in recording technique (sharp microelectrodes vs. patch pipettes) or the effects of anesthesia. On the other hand, genuine differences are likely to exist between the *in vitro* and *in vivo* conditions. For example, action-potential backpropagation could be differ-

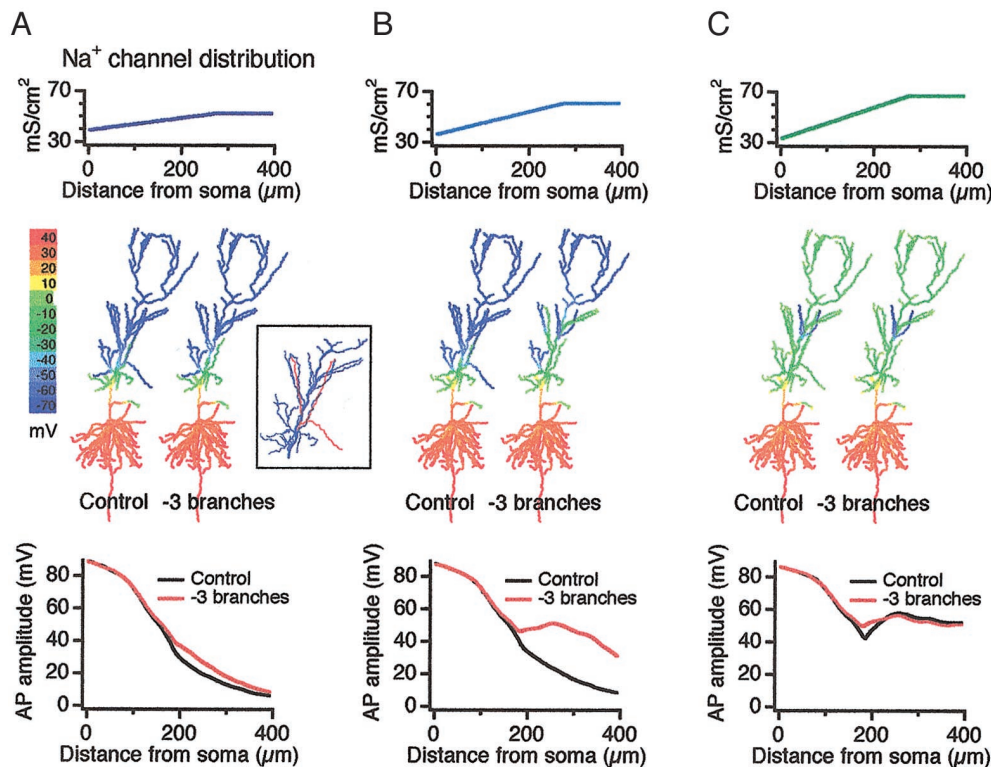


FIG. 10. Removal of a small number of dendritic side branches can induce strong propagation when weak backpropagating action potentials are close to threshold for active propagation. *A*: the spatial profile of action-potential backpropagation in control conditions and following removal of 3 side branches between 195 and 205  $\mu\text{m}$  from the soma. *Top*: the dendritic distribution of sodium channels. Delayed rectifying and A-type potassium channels are distributed as in Fig. 8A. *Middle*: color-coded display of voltage attenuation in neuron models containing a dendritic arbor that is intact (control) or with 3 oblique branches removed from the primary apical dendrite  $\sim 200 \mu\text{m}$  from the soma (-3 branches). *Inset*: "excised" branches are shown in red. *Bottom*: plot of action-potential amplitude as a function of distance along the primary apical dendrite for the 2 morphological conditions. Branch removal increases the amplitude of action potentials by only a few millivolts. *B*: the same model as in *A* only with a slightly steeper dendritic gradient of voltage-gated sodium channels. The format of panels is identical to that of *A*. In this model, removal of 3 branches converts weak propagation to strong propagation. *C*: a further incremental increase in the gradient of dendritic sodium channels results in strong propagation in both morphological conditions, showing that the striking effect of branch removal in *B* is restricted to a set of model parameters that gives rise to backpropagating action potentials that are close to the threshold for strong propagation.

entially attenuated in vivo by the increased shunting arising from the comparatively higher background of synaptic activity (Paré et al. 1998a,b). Indeed, it has been shown in vitro that when distal GABAergic inhibitory inputs are activated synchronously with electrical stimulation, action potentials in the distal dendrites may be strongly attenuated, typically at a discrete threshold of inhibition (Tsubokawa and Ross 1996). The same study showed that backpropagating action potentials could also be attenuated by membrane hyperpolarization produced by the recording electrode. We have observed a somewhat less pronounced voltage sensitivity in the amplitude of backpropagating action potentials, possibly as a consequence of differences in the morphology of recorded cells or in the way in which action potentials were generated (somatic current injection in the current study vs. antidromic stimulation). Relatively few inhibitory interneurons targeting distal dendrites in *s. lacunosum-moleculare* fire spontaneously in slices (Lacaille and Schwartzkroin 1988; Williams et al. 1994); it is thus unlikely that differences in the level of distal spontaneous inhibition between slices mediates the dichotomy in action-potential backpropagation observed in the present study.

#### Mechanisms controlling action-potential backpropagation

The initial shape of action potentials in the soma is highly correlated with the degree to which they subsequently attenuate in the distal dendrites. In 95% of paired somatic and distal dendritic recordings, values of somatic action-potential duration and maximum rate of rise in strong- and weak-propagating pyramidal neurons occupied nonoverlapping regions of continuous distributions, indicating that strong and weak backpropagation can be predicted with high accuracy based on the shape of the somatic action potential. Somatic action potentials in weak-propagating neurons were larger and faster rising than those in strong-propagating neurons, a surprising result given that a faster rise time and larger amplitude implies the presence of a larger underlying sodium current. However, action potentials in weak-propagating neurons were also shorter in duration, reflecting stronger repolarization by outward conductances. Although action potentials of shorter duration would be expected to be more sensitive to attenuation by membrane capacitance, it cannot be determined whether differences in action-potential shape identified in these experiments significantly influence dendritic propagation efficacy or whether the

two parameters are noncausally correlated. However, these results provide evidence that strong- and weak-propagating pyramidal neurons exhibit consistent differences in their electrophysiological properties that cannot be attributed to morphological variability.

Although the precise cellular mechanisms that confer weak versus strong backpropagation are not precisely known, we have gained insights into some of the important governing parameters by using relatively simple compartmental models. Manipulations of model parameters focused on sodium channels and A-type potassium channels based on previous demonstrations of their importance in regulating the amplitude of backpropagating action potentials in dendrites (Hoffman et al. 1997; Pan and Colbert 2001; Spruston et al. 1995). In our simulations, relatively subtle alterations in the somatodendritic distribution of either voltage-gated sodium channels or A-type potassium channels could interconvert modeled neurons between strong and weak action-potential backpropagation. Significantly, when systematic changes were made in the distribution of sodium or A-type potassium channels (leaving the distribution of the remaining 2 channel types constant), the resultant spatial profiles of action-potential amplitude exhibited a dichotomy at a discrete location in the primary apical dendrite, similar to our experimental data obtained from a population of neurons. In the models, only a narrow range of channel distributions gave rise to intermediate action-potential amplitudes in distal locations, consistent with the low frequency at which we observed intermediate action-potential amplitudes in the experimental data. An important aspect of the simulations is that the variance in the densities of sodium and A-type potassium channels distributed in modeled dendrites falls within the variance of densities that have been reported experimentally in CA1 pyramidal neurons (Hoffman et al. 1997; Magee and Johnston 1995). Thus while it is not known in what manner and to what extent voltage-gated channel densities vary in single neurons, our simple models demonstrate the principle that relatively minor differences in the spatial profile of channel expression can exert strong effects on action-potential backpropagation.

While our models focused on the effects produced by varying the densities of sodium and potassium conductances on distal action-potential backpropagation, it should be emphasized that a dichotomy in backpropagation efficacy might also arise from differential channel modulation in the dendrites. Both sodium and A-type potassium channels are modulated by the activity of protein kinases A and C (Cantrell et al. 1996, 1997; Colbert and Johnston 1998; Hoffman and Johnston 1998, 1999). In addition, a modeling study has shown that shifts in the activation range of A-type potassium channels of a magnitude that could be produced by modulators could in turn have significant effects on the distal extent of action-potential backpropagation (Migliore et al. 1999).

Neither the experimental data nor the modeling results rules out a role of dendritic structure in influencing whether a neuron exhibits weak or strong action-potential backpropagation. Although we observed no overall systematic differences in the diameter of the primary apical dendrite or branching complexity between labeled strong- and weak-propagating pyramidal

neurons, we did detect a small but significant local difference in the number of primary oblique branches ( $\leq 3$ ) in the region between 300 and 350  $\mu\text{m}$  from the soma, near where the dichotomy in the amplitude of backpropagating action potentials emerged. Our simulations showed that the removal of this small number of branches could switch action-potential backpropagation from weak to strong, but only when dendritic ion channel distributions were manipulated to render action-potential backpropagation close to, but just below threshold for active propagation. Based on the fact that the effects of branch removal were dependent on a specific set of model parameters, it seems unlikely that dendritic branching patterns alone can account for the dichotomy in action-potential backpropagation observed in the experimental data. Nevertheless, the spatial arrangement of dendritic branches must be considered as a potential influence.

#### *Implications for synaptic plasticity*

Temporally correlated patterns of excitatory postsynaptic potentials and backpropagating action potentials have been shown to be a robust stimulus for the induction of specific forms of synaptic plasticity in several areas of the brain (Bell et al. 1997; Bi and Poo 1998; Magee and Johnston 1997; Markram et al. 1997). The present finding that backpropagating action-potential amplitude and calcium influx is more robust in some pyramidal neurons suggests that these neurons might be more competent to undergo changes in synaptic efficacy in distal dendritic regions. It should be noted, however, that the regulation of backpropagating action-potential amplitude is dynamic under more physiologically complex conditions. During regular trains of action potentials, the amplitude in the distal dendrites of later backpropagating action potentials is comparable in both weak- and strong-propagating pyramidal neurons (e.g., Fig. 1, *B* and *C*, *right*). It has also been shown in both hippocampal CA1 pyramidal neurons and neocortical pyramidal neurons that the amplitude of backpropagating action potentials is enhanced when they occur in coincidence with appropriately timed subthreshold synaptic activity (Hoffman et al. 1997; Magee and Johnston 1997; Pan and Colbert 2001; Stuart and Häusser 2001). Some have stressed the importance of dendritic sodium channel activation in this amplification (Stuart and Häusser 2001), whereas others have argued for a role of dendritic A-type potassium channel inactivation (Hoffman et al. 1997; Pan and Colbert 2001). Thus *in vivo*, it is likely that the attenuation of backpropagating action potentials is regulated dynamically by fluctuations in the activation and inactivation state of voltage-gated sodium and potassium channels. As discussed above, the spatial pattern of inhibition adds another layer of complexity as well. As a result, the contribution of backpropagating action potentials to LTP induction in CA1 pyramidal neurons will depend not only on the relative timing of synaptic potentials and backpropagating action potentials but also on the temporal structure of their recent history of firing. Indeed, in neocortical pyramidal neurons, backpropagation efficacy and spike-triggered calcium influx is enhanced at certain frequencies of regular and irregular action-potential discharges (Larkum et al. 1999; Williams and Stuart 2000).

We thank Dr. Catherine Woolley for discussions and assistance regarding quantitative morphological analyses, T. Mickus for NeuroLucida reconstructions, and Drs. Martha Bohn and Bronwen Connor for the use of the NeuroLucida system. We also thank Drs. Valerie Kilman and Matthew Larkum for critical comments on the manuscript.

This work was supported by grants from the National Institute of Neurological Disorders and Stroke (NS-35180) and the Klingenstein Foundation to N. Spruston, the National Science Foundation (DMS-007510) to W. L. Kath, and by an individual National Research Service Award to N. L. Golding.

## REFERENCES

- ANDREASEN M AND LAMBERT JD. Regenerative properties of pyramidal cell dendrites in area CA1 of the rat hippocampus. *J Physiol (Lond)* 483: 421–441, 1995.
- BELL CC, HAN VZ, SUGAWARA Y, AND GRANT K. Synaptic plasticity in a cerebellum-like structure depends on temporal order. *Nature* 387: 278–281, 1997.
- BI GQ AND POO MM. Synaptic modifications in cultured hippocampal neurons: dependence on spike timing, synaptic strength, and postsynaptic cell type. *J Neurosci* 18: 10464–10472, 1998.
- BISCHOFBERGER J AND JONAS P. Action potential propagation into the presynaptic dendrites of rat mitral cells. *J Physiol (Lond)* 504: 359–365, 1997.
- CALLAWAY JC AND ROSS WN. Frequency-dependent propagation of sodium action potentials in dendrites of hippocampal CA1 pyramidal neurons. *J Neurophysiol* 74: 1395–1403, 1995.
- CANTRELL AR, MA JY, SCHEUER T, AND CATTERALL WA. Muscarinic modulation of sodium current by activation of protein kinase C in rat hippocampal neurons. *Neuron* 16: 1019–1026, 1996.
- CANTRELL AR, SMITH RD, GOLDIN AL, SCHEUER T, AND CATTERALL WA. Dopaminergic modulation of sodium current in hippocampal neurons via cAMP-dependent phosphorylation of specific sites in the sodium channel  $\alpha$  subunit. *J Neurosci* 17: 7330–7338, 1997.
- CHEN WR, MIDTGAARD J, AND SHEPHERD GM. Forward and backward propagation of dendritic impulses and their synaptic control in mitral cells. *Science* 278: 463–467, 1997.
- CHRISTIE BR, MAGEE JC, AND JOHNSTON D. Dendritic calcium channels and hippocampal long-term depression. *Hippocampus* 6: 17–23, 1996.
- COLBERT CM AND JOHNSTON D. Axonal action-potential initiation and  $\text{Na}^+$  channel densities in the soma and axon initial segment of subicular pyramidal neurons. *J Neurosci* 16: 6676–6686, 1996.
- COLBERT CM AND JOHNSTON D. Protein kinase C activation decreases activity-dependent attenuation of dendritic  $\text{Na}^+$  current in hippocampal CA1 pyramidal neurons. *J Neurophysiol* 79: 491–495, 1998.
- COLBERT CM, MAGEE JC, HOFFMAN DA, AND JOHNSTON D. Slow recovery from inactivation of  $\text{Na}^+$  channels underlies the activity-dependent attenuation of dendritic action potentials in hippocampal CA1 pyramidal neurons. *J Neurosci* 17: 6512–6521, 1997.
- GOLDSTEIN SS AND RALL W. Changes in action potential shape and velocity for changing core conductor geometry. *Biophys J* 14: 731–757, 1974.
- HÄUSSER M, STUART G, RACCA C, AND SAKMANN B. Axonal initiation and active dendritic propagation of action potentials in substantia nigra neurons. *Neuron* 15: 637–647, 1995.
- HINES ML AND CARNEVALE NT. The NEURON simulation environment. *Neural Comput* 9: 1179–1209, 1997.
- HOFFMAN DA AND JOHNSTON D. Downregulation of transient  $\text{K}^+$  channels in dendrites of hippocampal CA1 pyramidal neurons by activation of PKA and PKC. *J Neurosci* 18: 3521–3528, 1998.
- HOFFMAN DA AND JOHNSTON D. Neuromodulation of dendritic action potentials. *J Neurophysiol* 81: 408–411, 1999.
- HOFFMAN DA, MAGEE JC, COLBERT CM, AND JOHNSTON D.  $\text{K}^+$  channel regulation of signal propagation in dendrites of hippocampal pyramidal neurons. *Nature* 387: 869–875, 1997.
- JAFFE DB, JOHNSTON D, LASSER-ROSS N, LISMAN JE, MIYAKAWA H, AND ROSS WN. The spread of  $\text{Na}^+$  spikes determines the pattern of dendritic  $\text{Ca}^{2+}$  entry into hippocampal neurons. *Nature* 357: 244–246, 1992.
- JUNG HY, MICKUS T, AND SPRUSTON N. Prolonged sodium channel inactivation contributes to dendritic action potential attenuation in hippocampal pyramidal neurons. *J Neurosci* 17: 6639–6646, 1997.
- KAMONDI A, ACSADY L, AND BUZSAKI G. Dendritic spikes are enhanced by cooperative network activity in the intact hippocampus. *J Neurosci* 18: 3919–3928, 1998.
- KOESTER HJ AND SAKMANN B. Calcium dynamics in single spines during coincident pre- and postsynaptic activity depend on relative timing of back-propagating action potentials and subthreshold excitatory postsynaptic potentials. *Proc Natl Acad Sci USA* 95: 9596–9601, 1998.
- LACAILLE JC AND SCHWARTZKROIN PA. Stratum lacunosum-moleculare interneurons of hippocampal CA1 region. I. Intracellular response characteristics, synaptic responses, and morphology. *J Neurosci* 8: 1400–1410, 1988.
- LARKUM ME, KAISER KM, AND SAKMANN B. Calcium electrogenesis in distal apical dendrites of layer 5 pyramidal cells at a critical frequency of back-propagating action potentials. *Proc Natl Acad Sci USA* 96: 14600–14604, 1999.
- LINDEN DJ. The return of the spike: postsynaptic action potentials and the induction of LTP and LTD. *Neuron* 22: 661–666, 1999.
- LLINÁS R AND SUGIMORI M. Electrophysiological properties of in vitro Purkinje cell dendrites in mammalian cerebellar slices. *J Physiol (Lond)* 305: 197–213, 1980.
- MAGEE JC AND JOHNSTON D. Characterization of single voltage-gated  $\text{Na}^+$  and  $\text{Ca}^{2+}$  channels in apical dendrites of rat CA1 pyramidal neurons. *J Physiol (Lond)* 487: 67–90, 1995.
- MAGEE JC AND JOHNSTON D. A synaptically controlled, associative signal for Hebbian plasticity in hippocampal neurons. *Science* 275: 209–213, 1997.
- MAINEN ZF, JOERGES J, HUGUENARD JR, AND SEJNOWSKI TJ. A model of spike initiation in neocortical pyramidal neurons. *Neuron* 15: 1427–1439, 1995.
- MARKRAM H, LUBKE J, FROTSCHER M, AND SAKMANN B. Regulation of synaptic efficacy by coincidence of postsynaptic APs and EPSPs. *Science* 275: 213–215, 1997.
- MARTINA M, VIDA I, AND JONAS P. Distal initiation and active propagation of action potentials in interneuron dendrites. *Science* 287: 295–300, 2000.
- MICKUS T, JUNG H, AND SPRUSTON N. Properties of slow, cumulative sodium channel inactivation in rat hippocampal CA1 pyramidal neurons. *Biophys J* 76: 846–860, 1999.
- MIGLIORE M, HOFFMAN DA, MAGEE JC, AND JOHNSTON D. Role of an A-type  $\text{K}^+$  conductance in the back-propagation of action potentials in the dendrites of hippocampal pyramidal neurons. *J Comput Neurosci* 7: 5–15, 1999.
- PAN E AND COLBERT CM. Subthreshold inactivation of  $\text{Na}^+$  and A-type  $\text{K}^+$  channels supports the activity-dependent enhancement of back-propagating action potentials in hippocampal CA1 pyramidal neurons. *J Neurophysiol* 85: 1013–1016, 2001.
- PARÉ D, LANG EJ, AND DESTEXHE A. Inhibitory control of somatodendritic interactions underlying action potentials in neocortical pyramidal neurons in vivo: an intracellular and computational study. *Neuroscience* 84: 377–402, 1998a.
- PARÉ D, SHINK E, GAUDREAU H, DESTEXHE A, AND LANG EJ. Impact of spontaneous synaptic activity on the resting properties of cat neocortical pyramidal neurons in vivo. *J Neurophysiol* 79: 1450–1460, 1998b.
- POKORNY J AND YAMAMOTO T. Postnatal ontogenesis of hippocampal CA1 area in rats. I. Development of dendritic arborisation in pyramidal neurons. *Br Res Bull* 7: 113–120, 1981.
- SHOLL DA. Dendritic organization in the neurons of the visual and motor cortices of the cat. *J Anat* 87: 387–406, 1953.
- SPRUSTON N, SCHILLER Y, STUART G, AND SAKMANN B. Activity-dependent action potential invasion and calcium influx into hippocampal CA1 dendrites. *Science* 268: 297–300, 1995.
- STUART G AND HÄUSSER M. Initiation and spread of sodium action potentials in cerebellar Purkinje cells. *Neuron* 13: 703–712, 1994.
- STUART GJ AND HÄUSSER M. Dendritic coincidence detection of EPSPs and action potentials. *Nat Neurosci* 4: 63–71, 2001.
- STUART G, SCHILLER J, AND SAKMANN B. Action potential initiation and propagation in rat neocortical pyramidal neurons. *J Physiol (Lond)* 505: 617–632, 1997a.
- STUART G, SPRUSTON N, SAKMANN B, AND HÄUSSER M. Action potential initiation and backpropagation in neurons of the mammalian CNS. *Trends Neurosci* 20: 125–131, 1997b.
- SVOBODA K, DENK W, KLEINFELD D, AND TANK DW. In vivo dendritic calcium dynamics in neocortical pyramidal neurons. *Nature* 385: 161–165, 1997.
- TSUBOKAWA H, OFFERMANN S, SIMON M, AND KANO M. Calcium-dependent persistent facilitation of spike backpropagation in the CA1 pyramidal neurons. *J Neurosci* 20: 4878–4884, 2000.
- TSUBOKAWA H AND ROSS WN. IPSPs modulate spike backpropagation and associated  $[\text{Ca}^{2+}]_i$  changes in the dendrites of hippocampal CA1 pyramidal neurons. *J Neurophysiol* 76: 2896–2906, 1996.

- TSUBOKAWA H AND ROSS WN. Muscarinic modulation of spike backpropagation in the apical dendrites of hippocampal CA1 pyramidal neurons. *J Neurosci* 17: 5782–5791, 1997.
- VETTER P, ROTH A, AND HÄUSSER M. Propagation of action potentials in dendrites depends on dendritic morphology. *J Neurophysiol* 85: 926–937, 2000.
- WILLIAMS S, SAMULACK DD, BEAULIEU C, AND LACAÏLLE JC. Membrane properties and synaptic responses of interneurons located near the stratum lacunosum-moleculare/radiatum border of area CA1 in whole-cell recordings from rat hippocampal slices. *J Neurophysiol* 71: 2217–2235, 1994.
- WILLIAMS SR AND STUART GJ. Backpropagation of physiological spike trains in neocortical pyramidal neurons: implications for temporal coding in dendrites. *J Neurosci* 20: 8238–8246, 2000.
- YUSTE R AND DENK W. Dendritic spines as basic functional units of neuronal integration. *Nature* 375: 682–684, 1995.